Supplementary Information: Short-term exposure to fine particulate pollution and elderly mortality in Chile

Pablo Busch[1*], Paulo Rocha[2], Kyung Jin Lee[2], Luis Abdón Cifuentes[3], Xiao Hui Tai[4*]

[1*]Energy and Efficiency Institute, University of California, Davis, 1605 Tilia Street, Davis, 95616, CA, US.
[2]Department of Biostatistics, University of California, Davis, One Shields Avenue, Davis, 95616, CA, US.
[3]Department of Industrial and Systems Engineering, Pontificia Universidad Católica de Chile, Vicuña Mackenna 4860, Santiago, 7820436, Metropolitan, Chile.
[4]Department of Statistics, University of California, Davis, One Shields Avenue, Davis, 95616, CA, US.

*Corresponding author(s). E-mail(s): pmbusch@ucdavis.edu; xtai@ucdavis.edu;
Contributing authors: phrocha@ucdavis.edu; kjxlee@ucdavis.edu; lac@ing.puc.cl;

Supplementary Notes

Accuracy of satellite-based $PM_{2.5}$ estimates

Our analysis relies on satellite-based $PM_{2.5}$ estimates data produced by the Atmospheric Composition Analysis Group from the Washington University in St. Louis [1]. These data contain global estimates at a 0.01° (∼1.11 km) resolution at a monthly level from 1998 to 2021. They are calculated using satellite measurements of aerosol optical depth and a chemical transport model, and are calibrated using ground-based observations.

To validate the satellite data, we use publicly available $PM_{2.5}$ ground monitor data from Chile's National Air Quality Information System (SINCA). Chilean authorities periodically calibrate these monitor data with on-site filter measurements. Hourly or daily average $PM_{2.5}$ readings are available from multiple monitors across Chile; the geo-coordinates of each monitor are also available. The first monitor was installed in 2000, and monitor coverage has widely increased in recent years. In 2021, there were 61 monitors with validated data online. To validate the satellite-based estimates, we use data from a total of 59 monitors in the years 2015 to 2021. These years were selected since they had at least 50 monitors in each year with more than three-quarters of the days of $PM_{2.5}$ measurements available.

Methods. The first step is to aggregate daily monitor averages to a monthly level, for comparison with the monthly satellite-based data. We discard monitor-months with fewer than 24 days with official (validated) data in each month.

Next, we join the monitor data spatially with the satellite-based estimates. To assign a satellite-based $PM_{2.5}$ estimate to each monitor, we consider two methods. First, we use bilinear interpolation using the four raster cells that are closest to the monitor coordinates. Second, we use a point-in-polygon approach, simply locating the raster cell that each ground monitor is situated in. These two methods produced virtually identical results, and we present results from bilinear interpolation below. We compute the Pearson correlation coefficient and root-mean-square error (RMSE) between monthly $PM_{2.5}$ measurements for each ground monitor and the corresponding satellite estimate. We do this for all the data, and by year and region. Region is the first-level administrative division in Chile, containing multiple communes.

Results. Our constructed ground monitor data that we use as a baseline for comparison with satellite-based estimates, contains 3,858 monthly $PM_{2.5}$ measurements from 59 different monitor stations from January 2015 to December 2021. We find a strong linear correlation of 0.78 between satellite measurements and monitor ground data (SI Fig. S1). This correlation is consistent across the years analyzed, with minor differences. The RMSE between satellite-based and monitor estimates is 12.76 $\mu g/m^3$, and is consistent across the years.

All regions have correlations above 0.6, with the exception of three regions, regions XV, III, and XII. These three regions both have few monitors and low $PM_{2.5}$ concentrations. Region XI has a relatively high correlation coefficient of 0.78, but there are extreme values (SI Fig. S1) on the high end of the spectrum that are not being accurately captured by satellite estimates; these result in a high RMSE. Potential explanations for the poorer accuracy in these regions are (I) Monitors are not well calibrated nor maintained adequately. This could be because they are located where air pollution is not a major concern; or (II) satellite data is not well-adjusted or calibrated to detect lower $PM_{2.5}$ concentrations, which are present in the north of the country.

Overall, satellite-based estimates tend to be higher than ground measurements for lower concentrations (below 12 $\mu g/m^3$); the opposite applies for higher concentrations (above 50 $\mu g/m^3$), where satellite measurements are lower than monitor measurements.

Conclusion. Satellite-based measurements track ground measurements closely, and satellite-based data can considerably broaden the geographical and temporal coverage of $PM_{2.5}$ measurements, to areas without ground monitors. However, satellite measurements do not appear to be well-calibrated to detect $PM_{2.5}$ concentrations in the low and high ranges. This may lead to an upward bias in our estimates of the effect of $PM_{2.5}$ on mortality. To partially address this issue, we check the robustness of our results to the exclusion of the most problematic regions, regions XV, III, XI and XII.

Supplementary References

[1] Washington University in St. Louis. Surface $PM_{2.5}$: Global/Regional Estimates (V5.GL.03) (2021). URL https://sites.wustl.edu/acag/datasets/surface-pm2-5/. Data retrieved from, https://sites.wustl.edu/acag/datasets/surface-pm2-5/.

Supplementary Figures and Tables

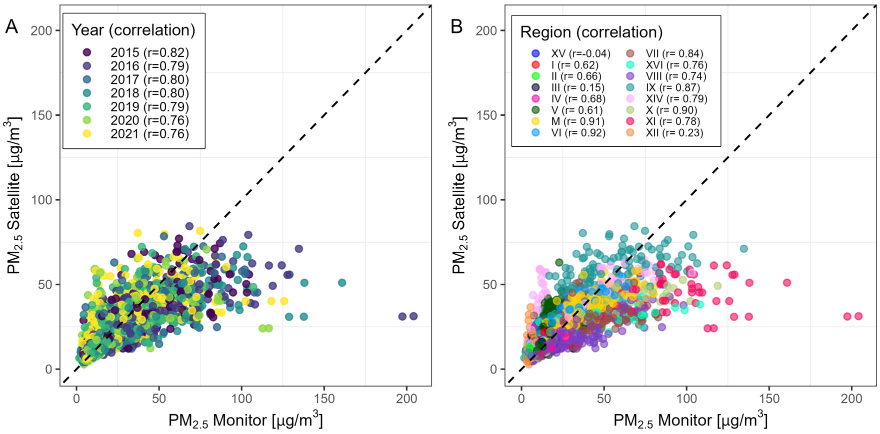

Fig. S1 Comparison of monthly $\mathbf{PM_{2.5}}$ monitor data against satellite data. Each dot represents a monthly average at each monitor location. The color shows either the year (A) or the region (B). The dashed line is the 45-degree line. The Pearson correlation coefficient is shown for each year (A) and region (B). For all periods and regions, there are 3,858 observations and the correlation is 0.78.

Table S1 Comparison of monthly $PM_{2.5}$ monitor data against satellite data. Number of months of observations (n), coefficient of determination (R^2) and root-mean-square error (RMSE) for each year and region (from North to South).

	n	R^2	RMSE
2015	434	0.67	12.57
2016	485	0.63	17.61
2017	511	0.64	11.85
2018	570	0.65	14.23
2019	612	0.62	9.96
2020	615	0.58	10.70
2021	631	0.57	12.03
Region XV	80	0.002	6.93
Region I	65	0.38	4.79
Region II	83	0.44	5.52
Region III	165	0.02	6.21
Region IV	156	0.46	4.50
Region V	224	0.37	10.18
Region M	717	0.82	6.39
Region VI	288	0.85	7.32
Region VII	421	0.71	12.68
Region XVI	162	0.58	16.48
Region VIII	587	0.55	10.73
Region IX	243	0.75	14.78
Region XIV	165	0.63	14.81
Region X	216	0.81	14.72
Region XI	208	0.61	32.61
Region XII	78	0.05	9.28
All	3858	0.61	12.76

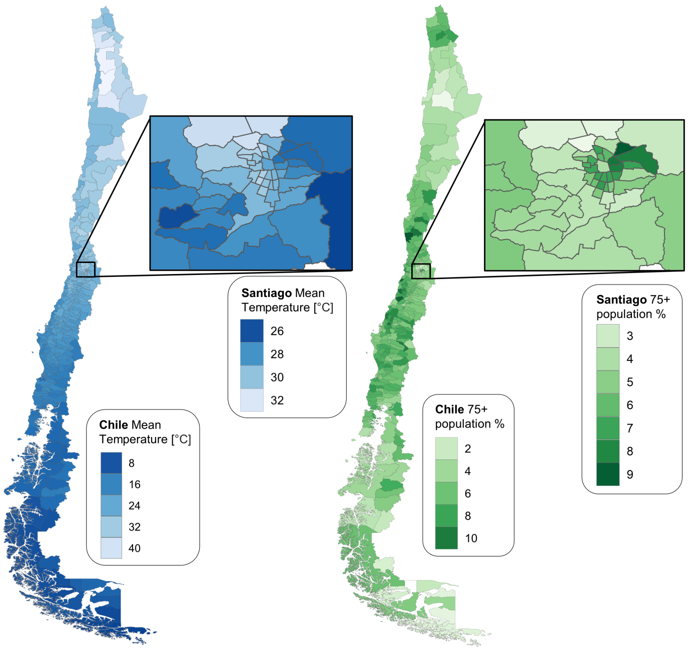

Fig. S2 Average land temperature [°C] and population shares of individuals aged 75 and older in 2019, for 327 communes in Chile. (Inset) The enlarged area shows part of the Metropolitan region (region M), including the capital city of Santiago.

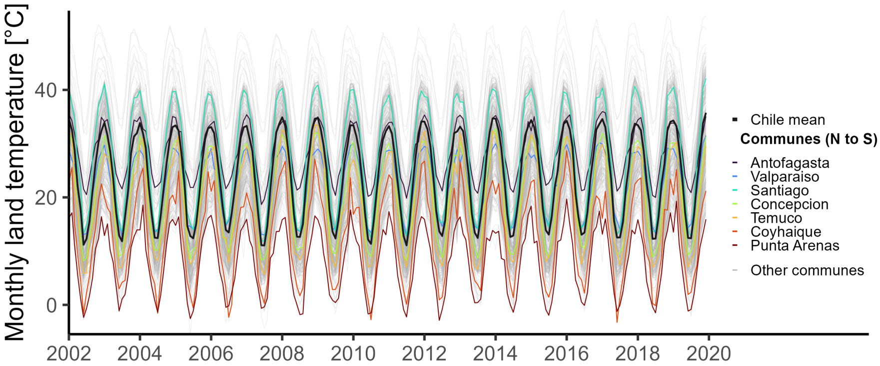

Fig. S3 Land temperature data. Monthly population-weighted land temperature from 2002 to 2019. Each line represents one of 327 communes. Representative communes across the country, ordered from north to south, are highlighted in different colors. Note that Chile is in the Southern Hemisphere.

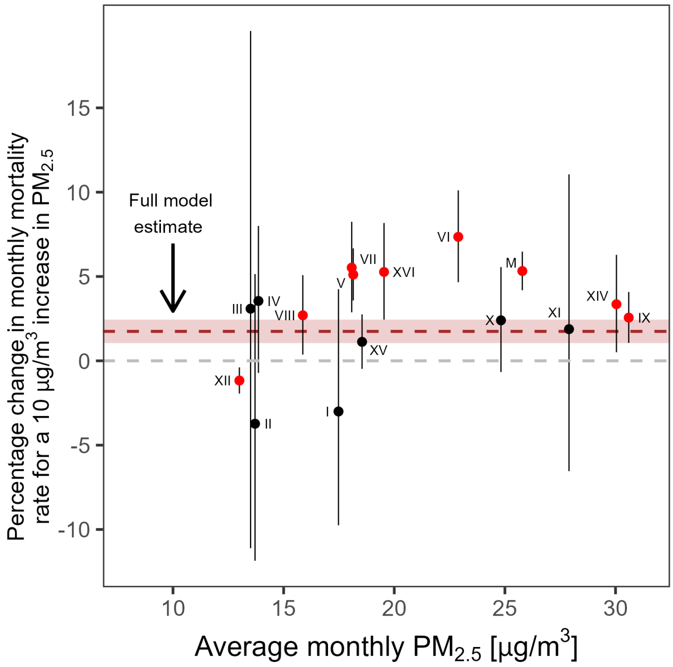

Fig. S4 Heterogeneous effects of $PM_{2.5}$ on 75+ mortality rate by region and air pollution levels. Estimates for each of the 16 regions in Chile, annotated using Roman numerals, plotted against the average monthly $PM_{2.5}$ for each region over the entire study period (2002-2019). Dots are point estimates and bars are 95% confidence intervals. A red dot indicates a significant effect, different from zero, at a 5% level. The red dashed line shows the main effect estimate (Fig. 2) and the red shaded band is the confidence interval. With the exception of region XV, all observations plotted to the right of region I are in the center-south part of the country.

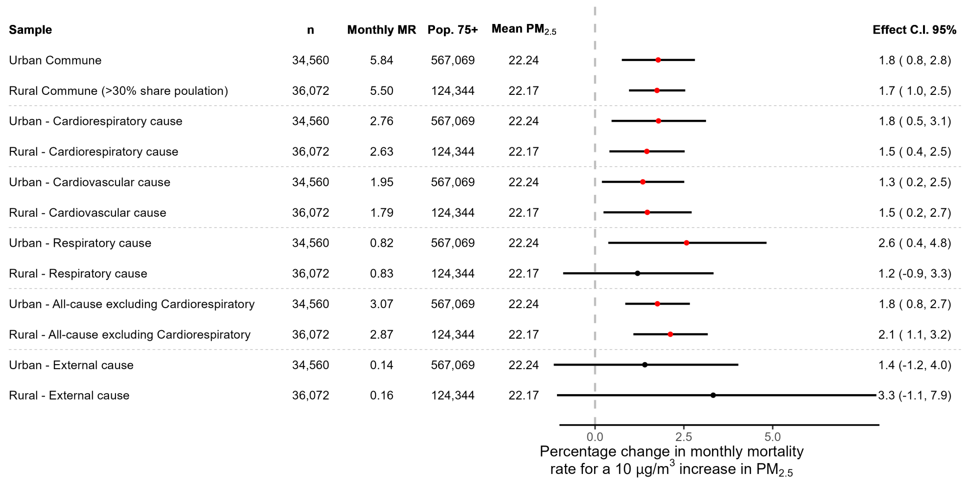

Fig. S5 Effect of $PM_{2.5}$ for urban and rural communes for different mortality causes for the 75+ age group. Each pair of rows shows models fitted for urban and rural communes, for different mortality causes, with information on the number of commune-month observations (n), average monthly mortality rate (monthly MR, deaths per 1,000 inhabitants), monthly 75+ population, mean $PM_{2.5}$ ($\mu g/m^3$, population-weighted), and the overall effect (black and red dots; red means statistically significant) with bars representing 95% CIs. External cause refers to all deaths not attributed to diseases, such as accidents or suicides. A commune is classified as rural if 30% or more inhabitants live in rural areas. Effects for urban and rural communes and very similar, with largest differences for respiratory causes.

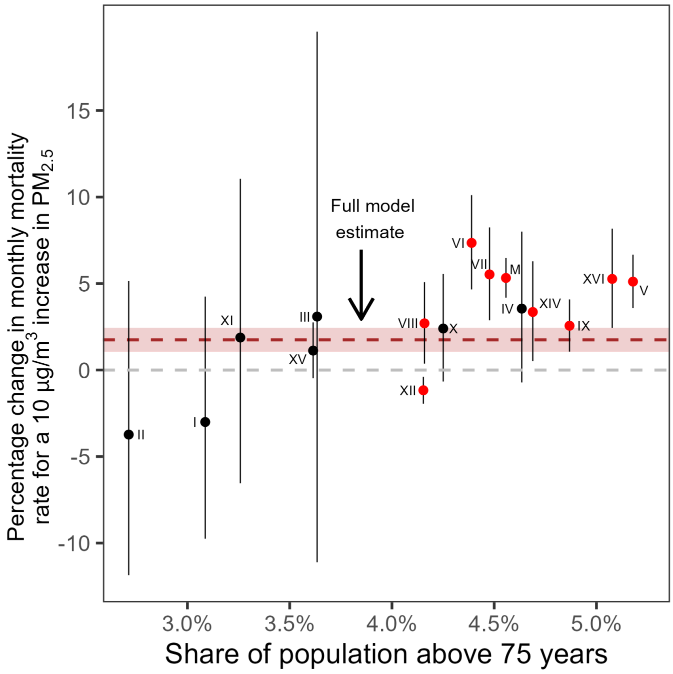

Fig. S6 Heterogeneous effects of $PM_{2.5}$ on 75+ mortality rate by region and share of 75+ population. Estimates for each of the 16 regions in Chile, annotated using Roman numerals, plotted against the average 75+ population share for each region over the entire study period (2002-2019). Dots are point estimates and bars are 95% confidence intervals. A red dot indicates a significant effect, different from zero, at a 5% level. The red dashed line shows the main effect estimate (Fig. 2) and the red shaded band is the confidence interval. All observations with share of 75+ larger than 4% are in the center-south of the country, with the exception of region IV.

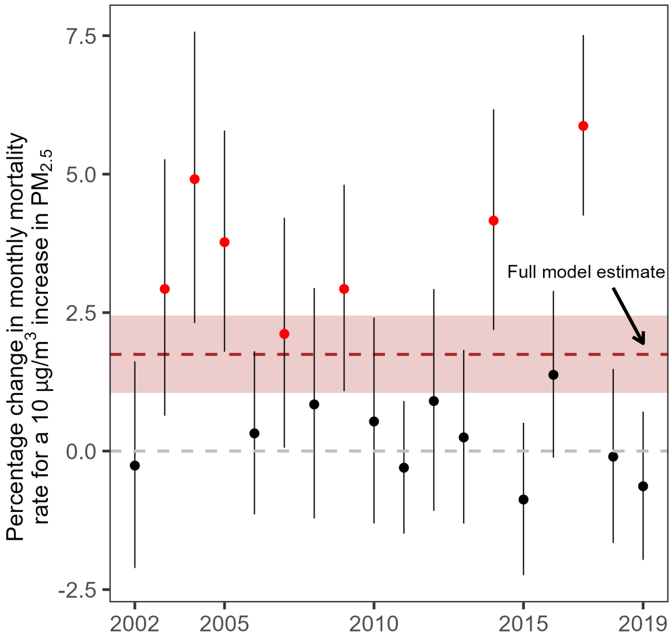

Fig. S7 Estimated effects over time. Effects are estimated separately for each year of data, from 2002 to 2019. Dots are point estimates and bars are 95% confidence intervals. A red dot indicates a significant effect, different from zero, at a 5% level. The red dashed line shows the main effect estimate (Fig. 2) and the red shaded band is the confidence interval.

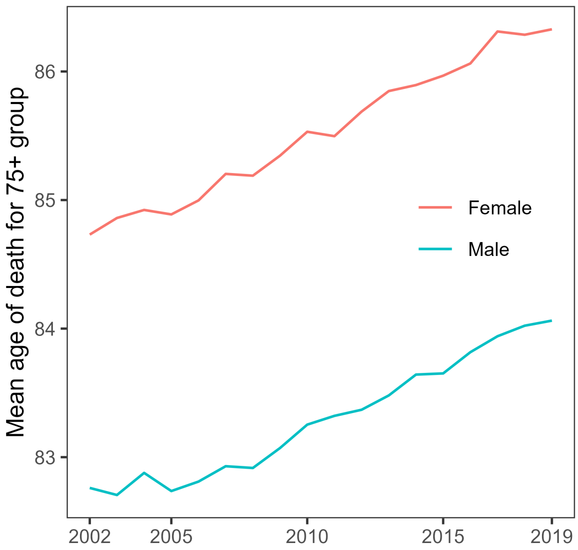

Fig. S8 National (Chile) mean age of death for the 75+ group by year and sex.

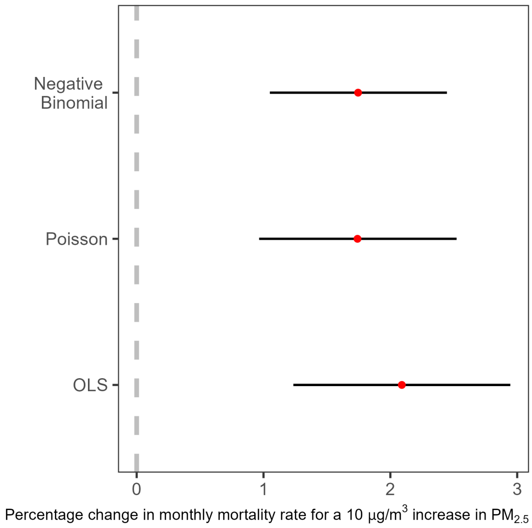

Fig. S9 Comparison of the estimated coefficients under different model families. To check the robustness of our results to modeling assumptions, we consider Poisson and ordinary least squares (OLS) models instead of the negative binomial model that was presented in the main results. All three models, negative binomial, Poisson, and OLS, show virtually identical results. A red dot indicates a significant effect at 5% level.

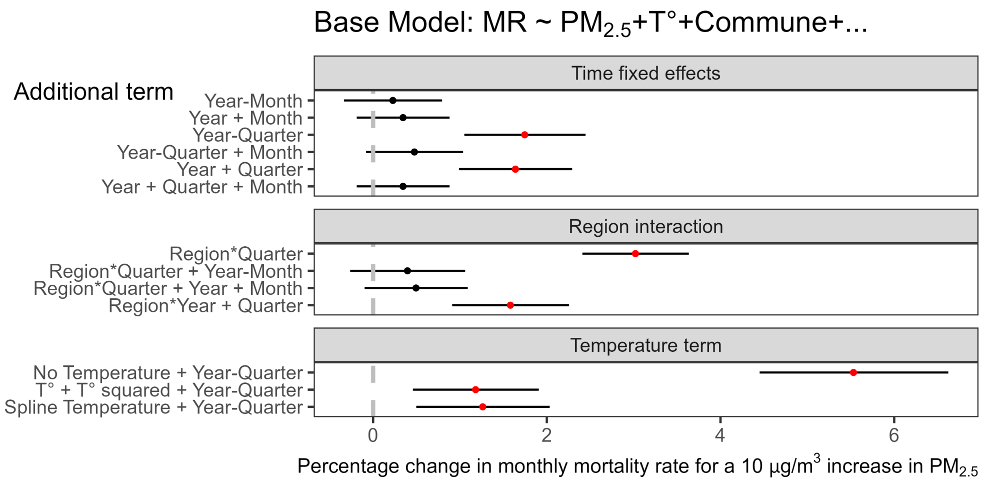

Fig. S10 Comparison of the estimated effect under different model specifications. Instead of quarter-year fixed effects, we consider the more restrictive month-year fixed effect, and other variations of month fixed effects. While these more restrictive fixed effects improve the identification of the causal effect, they absorb most of the variation in $PM_{2.5}$, thus diminishing its observable effect on mortality. While estimates remain positive, they are not statistically significant. We also consider more flexible fixed effects that vary by region, and different functional forms for the temperature variable. Removing temperature, a confounding variable, increases the relative risk of $PM_{2.5}$ to around 6%. Including a squared temperature term or spline specification for temperature with 3 degrees of freedom results in a positive estimate of around 1.2%.

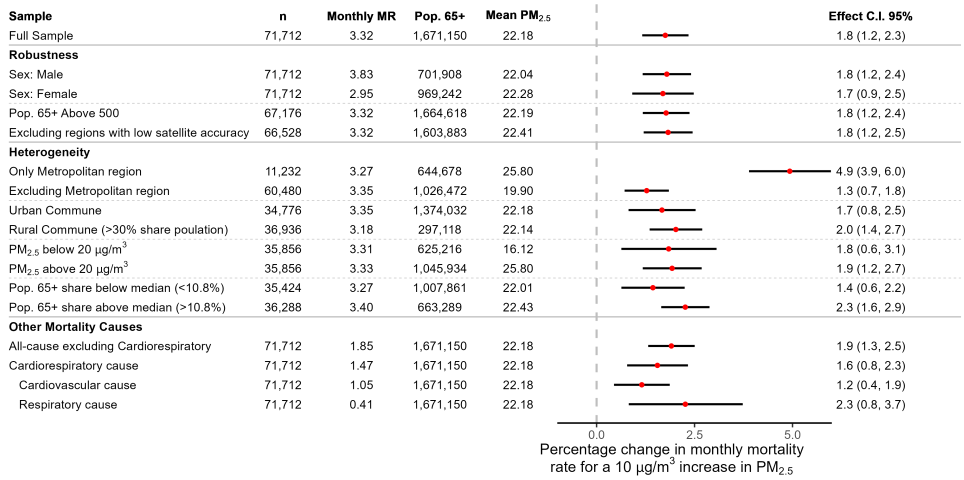

Fig. S11 Effect of $PM_{2.5}$ for the full sample and for various subgroups for the 65+ age group. Each row shows a model fitted for a different subgroup, with information on the number of commune-month observations (n), average monthly mortality rate (monthly MR, deaths per 1,000 inhabitants), monthly 65+ population, mean $PM_{2.5}$ ($\mu g/m^3$, population-weighted), and the overall effect (black and red dots; red means statistically significant) with bars representing 95% CIs. External cause refers to all deaths not attributed to diseases, such as accidents or suicides. Results for the 65+ age group are almost identical to the main analysis for individuals 75+. Note that the base mortality rates for 65+ are much lower than for 75+, suggesting that a large number of deaths of the 65+ group occur in individuals 75 and older.

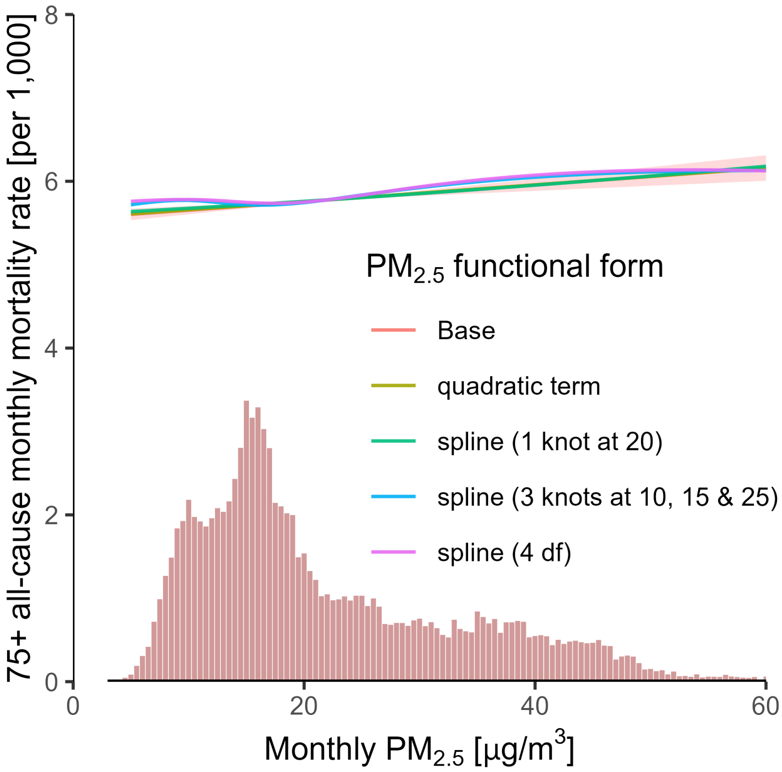

Fig. S12 Response function using more flexible functional forms for $\mathbf{PM_{2.5}}$. We consider quadratic and spline terms for $PM_{2.5}$ exposure, instead of the linear (Base) model (shaded band is the 95% confidence interval) that was presented in the main results. These more flexible models result in roughly the same shaped response function as linear models, particularly in regions where majority of the data lie (84% of the data have $PM_{2.5}$ exposures exceeding $10\mu g/m^3$).